LOW-ENERGY IMPACT INDUCED DAMAGE IN CARTILAGE: A MULTISCALE MODELING STUDY USING FE2M

Kosar Safari (1), Ashkan Almasi (1), Phoebe Szarek (2), David M. Pierce (1,2)

(1) School of Mechanical, Aerospace, and Manufacturing Engineering, University of Connecticut, Storrs, CT, USA (2) Department of Biomedical Engineering, University of Connecticut, Storrs, CT, USA

INTRODUCTION

Osteoarthritis (OA) remains a prevalent and incapacitating ailment with the degeneration of cartilage as a hallmark feature. The underlying causes and anticipated progression of OA remain unknown.

While microcracks in bone have been characterized extensively [1], and sub-millimeter-scale surface fissures are well known for early to advanced osteoarthritis (OA) [2], we recently demonstrated that low-energy impact usually considered non-injurious can in fact cause micrometer-scale cracks in the collagen network of human cartilage [3,4]. Pre-clinical OA may originate with microcracks in the network of collagen, and propagation of these microcracks within the extracellular matrix (ECM) may initiate a cascade of degeneration towards OA . However, the mechanisms of initiation and propagation of microcracks under mechanical loads to cartilage during normal daily activities remains unknown.

We aim to elucidate mechanical damage to collagen and collagen networks in cartilage by leveraging our experimental results and multiscale computational modeling. We simulated, using our custom FE2M modeling framework implemented in FEBio [5], unconfined compression of cartilage explants. We employed Statistically Equivalent Representative Volume Elements (SERVEs) [6] within the superficial zone, while we used standard FE the remaining cartilage volume (middle and deep zones) [7]. We validated the global results of our FE2M simulations by comparing predictions with those recently measured experimentally by us [3]. To better understand our predictions we performed: (1) sensitivity analysis on the modeling framework to quantify prediction sensitivity to input material parameters, and (2) tested stretch and stress within individual collagen fibers as predictors of collagen failure.

METHODS

Experimental Evidence. In previous experiments we examined 76 cylindrical osteochondral plugs (diameter = 3 mm and average thickness = 1.318 mm) [3]. We divided specimens into two low-energy impact groups: low impact (LI) = 1.5-2.5 mJ/mm³ and high impact (HI): 2.5-4.0 mJ/mm³). The impact velocity was $V_{\rm imp} = 0.5$ m/s, the drop height (h) was $(V_{\rm imp})^2/2g$, and the energy impact $(E_{\rm imp})$ was mgh/V based on

our experimental data, with V the volume of the specimen and g the acceleration constant. We determined the force for impact loading (F) using $F = 2E_{\rm imp}(V/(V_{\rm imp})^2)g$. In another study we established the minimum impact energy capable of inducing microcracks in cartilage [4]. From these data we had a third data set corresponding to a maximum impact (MI).

We also independently established the median failure stress for collagen fibers as $41.0\,\mathrm{kPa}$, the maximum failure stress as $47.3\,\mathrm{kPa}$, and the minimum failure stress at $35.8\,\mathrm{kPa}$, along with a median failure stretch as $2.4\,\mathrm{[6]}$.

FE2M Modeling Framework. We recently established a 3-D multiscale framework in FEBio which we called FE2M, integrating mixture theory and finite elements for solving two-scale, nonlinear, coupled, and timedependent boundary value problems (BVPs) in poro-hyperelastic, fluidsaturated porous media [6]. To solve the governing macroscopic partial differential equations we employ the finite element method twice. Initial macroscopic quantities, obtained from an intermediate solution of the macroscopic FE model, serve as boundary conditions on the microscopic Representative Volume Elements (RVEs or SERVEs). These include the deformation gradient $\overline{\mathbf{F}}_{S}$ and the gradient of pressure times the fluid volume fraction $\nabla(\overline{n^{\rm F}p})$. After solving the microscopic FE model with these BCs, we evaluate the macroscopic material tangent \overline{A} and measures \overline{P} , $(\mathbf{E}_S)_S' \cdot \mathbf{C}_S J_S$, $n^F \mathbf{w}_{FS}$ at each Gauss integration point through volume averaging of the underlying RVE. We use homogenization of any microscale quantity • over an RVE or a representative surface element to calculate its macroscopic counterpart $\bar{\bullet}$ using 1, where V_{0S} and A_{0S} are reference volumes and areas, respectively,

$$\langle \bar{\bullet} \rangle = \frac{1}{V_{0\mathrm{S}}} \int_{\mathcal{B}_{0\mathrm{S}}} \bullet \mathrm{d}V_{0\mathrm{S}}, \quad \lfloor \bar{\bullet} \rfloor = \frac{1}{A_{0\mathrm{S}}} \int_{\mathcal{B}_{0\mathrm{S}}} \bullet \mathrm{d}A_{0\mathrm{S}}. \tag{1}$$

Statistically Equivalent Representative Volume Elements. Leveraging information on the orientation, diameter, and volume fraction of type II collagen fibers within the superfacial zone [8], we generated SERVEs, and used them in the superficial zone of cartilage within our FE2M framework. We included discrete fibers as nonlinear springs, and modeled the

interfibrillar space using a biphasic, neo-Hookean model. We used a twoparameter power law function of stretch to model networked fiber of type II collagen as [6],

$$\Psi = c_1(\sqrt{I_4} - 1)^{c_3}, \ \sigma = \lambda c_1 c_3(\lambda - 1)^{(c_3 - 1)}, \tag{2}$$

where c_1 [MPa] and c_3 [—] are model parameters, I_4 is the fourth pseudo-invariant, and λ is the fiber stretch.

Boundary Value Problem. We modeled a 3-D 2° wedge of the cylindrical plug of cartilage with a diameter of 1.5 mm and a thickness of 1.318 mm. In Fig. 1(a) we show a schematic of the model with boundary conditions. We fixed the central node in the x-, y-, and z-directions, and the bottom surface of the model was fixed in the z-direction.

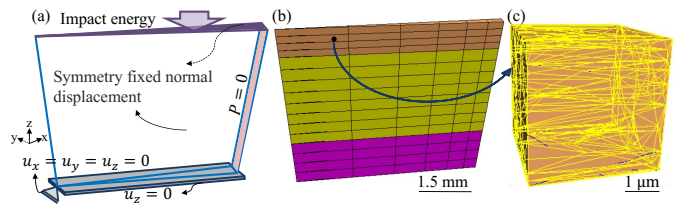


Figure 1: Boundary value problem for cartilage impact and corresponding FE models: (a) schematic of 2° cartilage wedge; (b) mesh of macroscopic structure; (c) SERVE with statistically equivalent orientation, dispersion, and volume fraction of collagen fibers.

We set the fluid pressure to zero on the radial surface, while all other surfaces had flux equals zero. To model impact, we applied a force to a rigid plate placed on top of the cartilage, establishing a contact between the top surface of the cartilage and the plate. Subsequently, we applied forces of $0.08~\rm N$, $0.16~\rm N$, and $0.20~\rm N$ with a linear ramp from zero to 1 ms for LI, HI, and MI, respectively. In Fig. 1(b) we show the corresponding mesh used in the two-scale model, while in Fig. 1(c) we illustrate a representative SERVE with statistically equivalent orientation, dispersion, and volume fraction of collagen fibers.

Predictions of Collagen Failure and Microcracking. We concentrate on microcrack density (experimental) and the ratio of failed fibers (computational) as a key parameters for comparison between our experiment and simulation results. Microcrack density is the number of microcracks per unit area #/mm² measured in experiments. In our numerical model, we introduced the ratio of failed fibers (number of failed fibers/total number of fibers) to quantify the proportion of failed fibers to the total number of fibers. We established a custom algorithm to identify failed fibers – we compare the stress and stretch of calculated for each fiber to the critical values and then calculates the ratio of failed fibers.

Sensitivity Analyses. We conducted sensitivity analyses on the parameters of the constitutive model for collagen fibers to assess the influence on both macroscopic and microscopic results. To this end we implemented a Monte Carlo sampling method for the random selection of c_1 within the range [3.82-7.82] MPa and c_3 within the range [3.568-4.072].

RESULTS

In Fig. 2 we show results for the macroscopic structure of cartilage and representative Element 76 for HI.

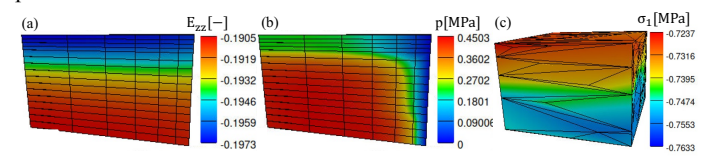


Figure 2: Macroscale and Microscale results for high impact energy: (a) z-strain; (b) fluid pressure; (c) first principal stress for element 76.

In Fig. 2(a) we show the strain within the cartilage specimen at peak load the Z-direction, and in Fig. 2(b) the interstitial fluid pressure. In Fig. 2(c) we show the first principle stress for element 76, which is in the center of the superficial zone.

Utilizing our SERVEs in the superficial zone, we determined the stretch and corresponding stress for each fiber during the impact events. In Fig. 3 the first row shows histograms of the distributions of fiber stretch under LI, HI, and MI, while in the second row we show corresponding histograms of the distributions of fiber stress for the same three tests.

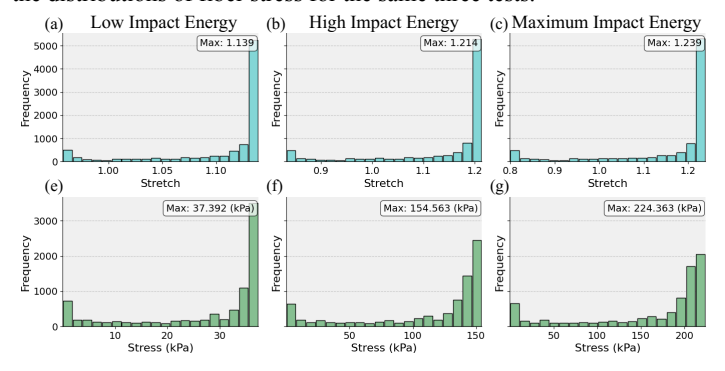


Figure 3: Distributions of stretch and stress for LI, HI, and MI.

Using stress as a predictor of fiber failure, we calculated the ratio of failed fibers as 34.8%, 73.0% and 75.3%, for for LI, HI, and MI respectively. The corresponding experimental values for microcrack density were 2.34 for LI and 3.25 for HI, indicating that microcracks did appear in these impact conditions. Stretch was not a predictor of fiber failure.

In Fig. 4 we show the convergence of the global model with respect to the parameters used to model the stretch-stress response of the collagen fibers (2).

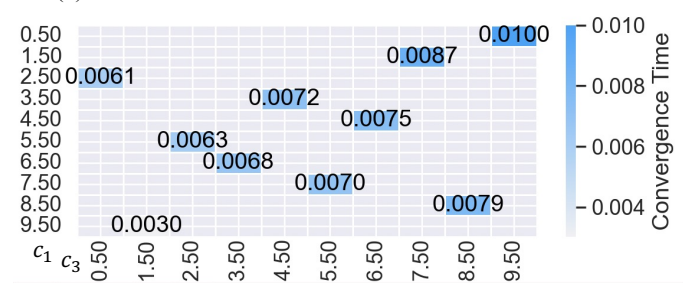


Figure 4: Model sensitivity to constitutive model parameters.

We note that there are combinations of c_1 and c_3 for which the global model will not converge while ramping to the maximum impact load. Additionally, the mechanical response of the global model varies with variations in parameters of the constitutive model for collagen fibers.

DISCUSSION

We present macroscopic and microscopic results for three different impact loadings of cartilage. Our results provide preliminary insights into the mechanical and failure behaviors of type II collagen. Utilizing our SERVEs, we conclude that stress may be a predictor of fiber failure, but stretch is likely not. Sensitivity analyses on constitutive model parameters for collagen reveal their significant impact on the mechanical response of cartilage.

ACKNOWLEDGEMENTS

NSF CAREER 1653358, UConn GTA Fellowship.

REFERENCES

[1] Martin, R, Bone, 30:8-13, 2002. [2] Repo, RU et al., J Bone Joint Surg Am, 59(8):1068-1076, 1977. [3] Santos, S et al., Osteoarthritis Cartilage, 27:1392–1402, 2019. [4] Kaleem, B et al., Osteoarthritis Cartilage, 25:544–553, 2017. [5] Almasi, A et al., submitted for review. [6] Szarek, P, PhD Thesis, University of Connecticut, 2023. [7] Pierce, DM et al., Biomech Model Mechanobiol, 15:229–244, 2016. [8] Szarek, P et al., Osteoarthritis Cartilage Open, 2:100086, 2020.